

Title	Radiation Resistivity of Pure Silica Core Image Guides under Intermittent Irradiation Tests
Author(s)	Okamoto, Shinichi; Onishi, Tokuhiko; Kanazawa, Tamotsu; Tsuji, Yukio ; Hayami, Hiroyuki; Zushi, Toshihiro; Akutsu, Takeji
Editor(s)	
Citation	Bulletin of University of Osaka Prefecture. Series A, Engineering and natural sciences. 1993, 42(1), p.109-121
Issue Date	1993-12-01
URL	http://hdl.handle.net/10466/8581
Rights	

Radiation Resistivity of Pure Silica Core Image Guides under Intermittent Irradiation Tests

Shinichi OKAMOTO*, Tokuhiro OHNISHI*, Tamotsu KANAZAWA*,
Yukio TSUJII*, Hiroyuki HAYAMI**, Toshihiro ZUSHI** and Takeji AKUTSU**

(Received June 30, 1993)

Image guides are widely used in industry today. Especially pure-silica-core image guides are becoming increasingly popular in nuclear environments, where its superior radiation resistivity allows remote visual inspection. Therefore, we have been studying to increase the radiation resistivity of pure-silica-core image guides. The radiation resistivity is mainly determined by the core material, and generally, OH-doped cores are considered to be the best. However, our experiments revealed that F-doped, OH-free cores had better radiation resistivity than OH-doped cores. We performed the intermittent ^{60}Co -gamma-ray irradiation test in which irradiation recovery phases were repeated three times. The results were compared with results from the continuous irradiation test. Four kinds of pure-silica-core image guide samples, using F, F+OH, OH and Cl+OH doped cores, were tested under four different dose rates. The results clearly revealed that the F-doped core was the most superior. At any dose rate and total dose, the superiority of core dopant was in the order $F > F+OH > OH > Cl+OH$.

1. Introduction

There are a number of reports on how the dopant of a core affects the radiation resistivity of optical silica fibers.^{1),2)} According to these reports, OH-doped, Cl-free core fibers have excellent resistivity.^{3),4)} In contrast to these reports, our study on ways to improve radiation resistivity revealed that the resistivity of image guides using F-doped, OH-free cores were much better.⁵⁾ We have discovered that F yields better radiation resistivity than OH which has been known for its ability to suppress radiation deterioration. We have already reported the effects that F, Cl and OH have on the radiation resistivity of image guides during 50 hours of continuous irradiation.⁶⁾ Therefore, using the same samples F, OH, Cl+OH and F+OH as before, we performed three intermittent irradiations, and then compared the results with that of a continuous irradiation.

* Research Center of Radiation, Research Institute for Advanced Science and Technology

** Mitsubishi Cable Industries, Ltd.

2. Experiments

2.1 Samples

The pure-silica-core image guide is composed of multiple glass fibers each having a three-layer preform structure, as shown in Fig. 1 (a). Each fiber is arranged precisely in a silica tube then bundled and drawn into fused image guides. This forms what is called the multiple fiber image guide, in which the glass fibers (pixels) are united with each other. The pixels in our image guides are beautifully arranged as shown in Fig. 1(b). The core of image guides has the greatest influence on the radiation resistivity. The five samples, A, B, C, D and E listed in Table 1 were selected on the basis of our previous experimental results. All of the samples have a support layer which consists of a synthetic silica material. The image guides each contain 3,000 pixels.

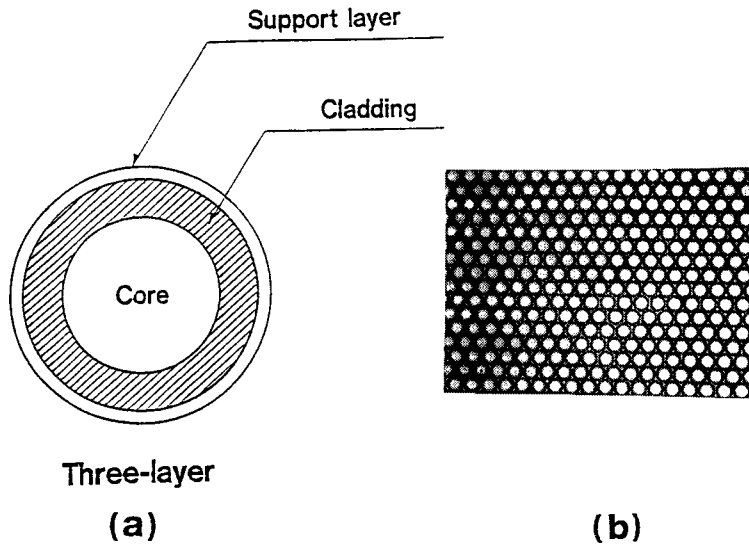


Fig. 1 (a): Preform structure and (b): magnified cross-section of image guide.

Table 1 Image guide samples for irradiation tests

Sample	Core material			Preform structure	Number of picture elements
	Cl content (ppm)	OH content (ppm)	F content (ppm)		
A	Free	Free	3,500	Three-layer	3,000
B	Free	Free	4,500		
C	Free	750	Free		
D	1,700	30	Free		
E	Free	100	1,500		

2.2 Irradiation test

The irradiation test was performed as shown in Fig.2, using a ^{60}Co radiation source. The white light source was connected to one end and the light output power from the other end was measured between the wavelength of 400-700nm by a spectroscope. Radiation induced losses were calculated from the difference of light output power before and after the irradiation.

Table 2 shows the irradiation test conditions for pure-silica-core image guides. At a constant dose rate, irradiation was repeated three times with intervals in between.

The length of the intervals was made long enough for the samples to recover before next irradiation.

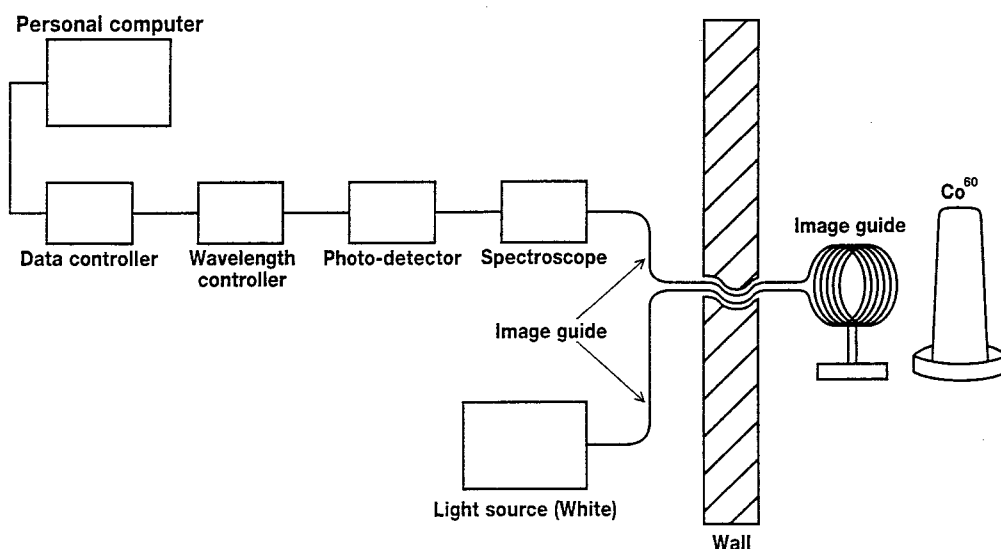


Fig. 2 Irradiation test diagram.

Table 2 Irradiation test conditions

Dose rate (C/kg·h)	Consecutive irradiated time in the first test (hrs)	Intermission between the first test and the second test (hrs)	Consecutive irradiated time in the second test (hrs)	Intermission between the second test and the third test (hrs)	Consecutive irradiated time in the third test (hrs)
5.16 2×10^4 R/h	50	1,300	50 (total 100)	650	74 (total 174)
5.16×10 2×10^5 R/h	50	1,300	50 (total 100)	650	74 (total 174)
1.29×10^2 2×10^6 R/h	26	1,250	50 (total 76)	650	74 (total 150)
2.58×10^2 2×10^6 R/h	26	1,250	50 (total 76)	650	74 (total 150)

3. Results

3.1 Core material dependence of radiation-induced losses

Using the samples shown in Table 1, the irradiation tests were performed under four different dose rates. The induced loss vs. wavelength characteristics showed similar movements in all of the image guides, regardless of the dose rates. Therefore, in this report, we focus only on the 5.16×10^4 C/(kg·h) dose rate, and discuss the induced loss vs. wavelength characteristics. Figs. 3(a)-3(b), Figs. 4(a)-4(c), and Figs. 5(a)-5(c) show the changes made during the three repeated irradiations and the recovery periods. The order of radiation resistivity superiority during repeated irradiation is A, B, E, C and D. From this order, it is obvious that both samples A and B which are only doped with F, are superior to the rest. Next in order is sample E, and it is also obvious that the sample has the characteristics of both F and OH. Between the 400-500 nm range, sample D suffers an extremely high radiation-induced loss compared to sample C, thus indicating that sample C is superior to sample D in the whole visible wavelengths. Samples C and E which have OH-doped cores, have absorption peaks at about 480 nm and 600 nm wavelengths. These results demonstrate the importance of core materials in pure silica image guides on resisting radiation. From Figs. 3-5, we can compare the movement of the induced loss during irradiation and

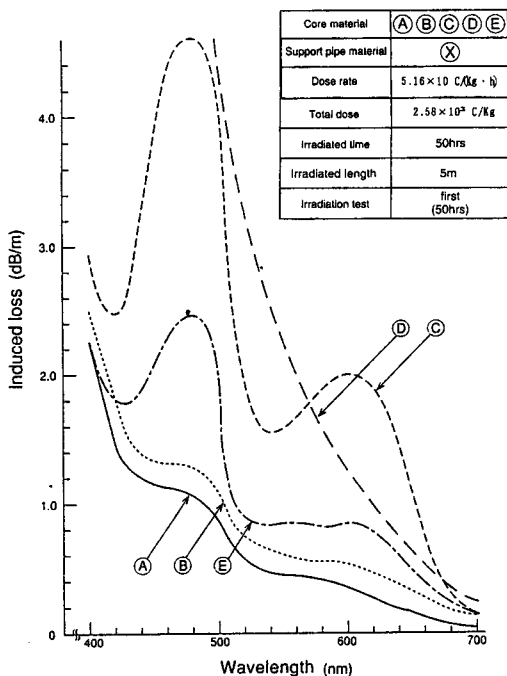


Fig. 3(a) Core materials dependence of radiation-induced losses of image guides when the 1st irradiation test (50 hours) was finished.

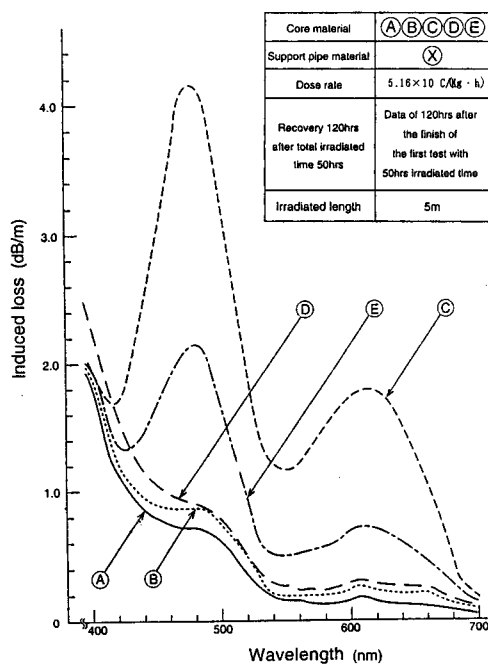


Fig. 3(b) Core materials dependence of radiation-induced losses of image guides after 120 hours from the end of the 1st irradiation test (50 hours).

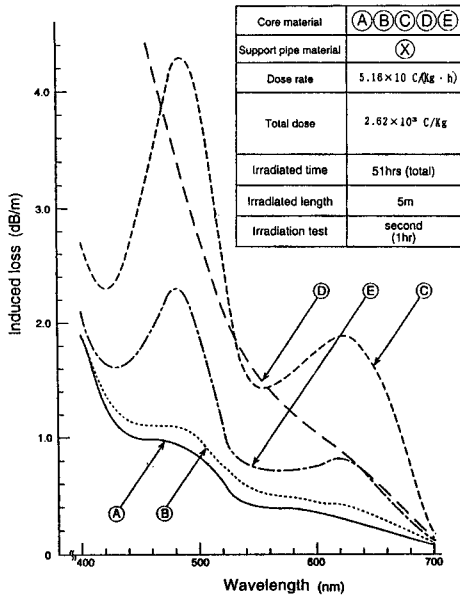


Fig. 4(a) Core materials dependence of radiation-induced losses of image guides when the 2nd irradiation of 1 hour, which began after 1,300 hours from the end of the 1st irradiation, was finished.

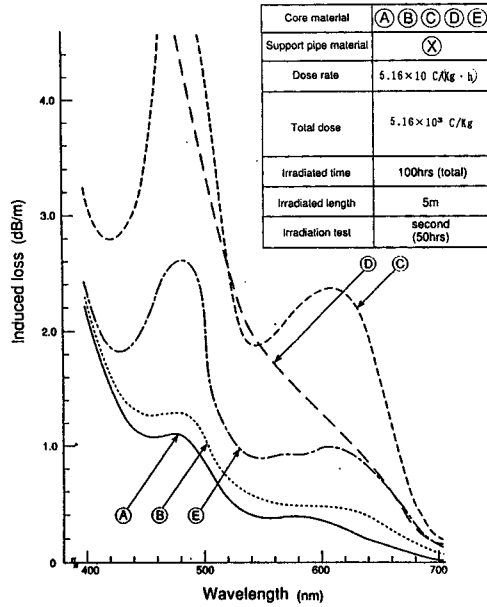


Fig. 4(b) Core materials dependence of radiation-induced losses of image guides when the 2nd irradiation of 50 hours, which began after 1,300 hours from the end of the 1st irradiation, was finished.

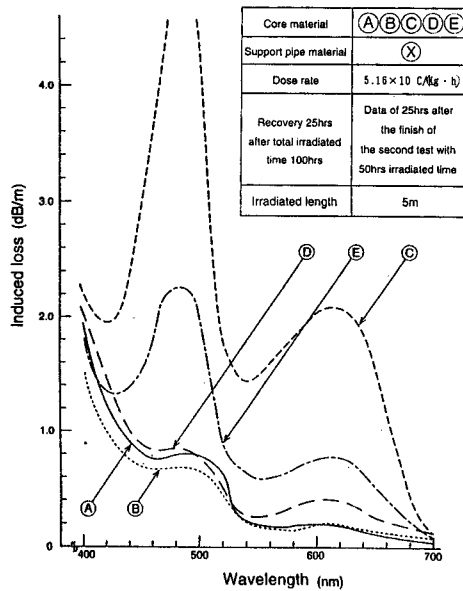


Fig. 4(c) Core materials dependence of radiation-induced losses of image guides after 25 hours from the end of the 2nd irradiation test (total irradiated time 100 hours).

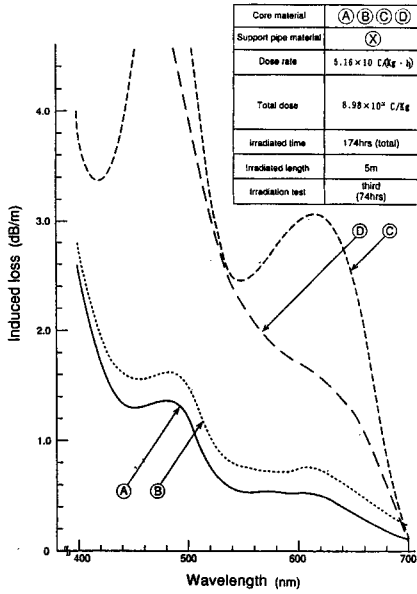


Fig. 5(a) Core materials dependence of radiation-induced losses of image guides when the 3rd irradiation of 74 hours, which began after 650 hours from the end of the 2nd irradiation, was finished.

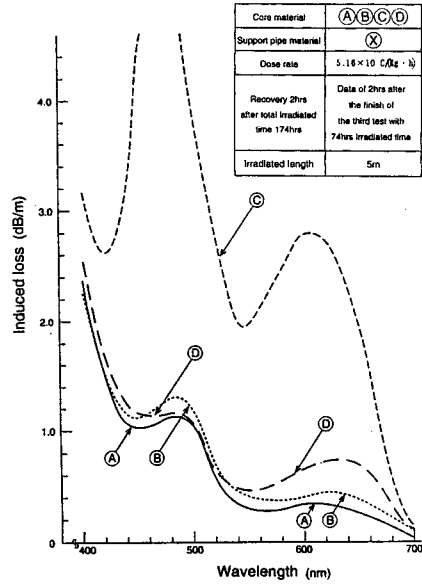


Fig. 5(b) Core materials dependence of radiation-induced losses of image guides after 2 hours from the end of the 3rd irradiation test (total irradiated time 174 hours).

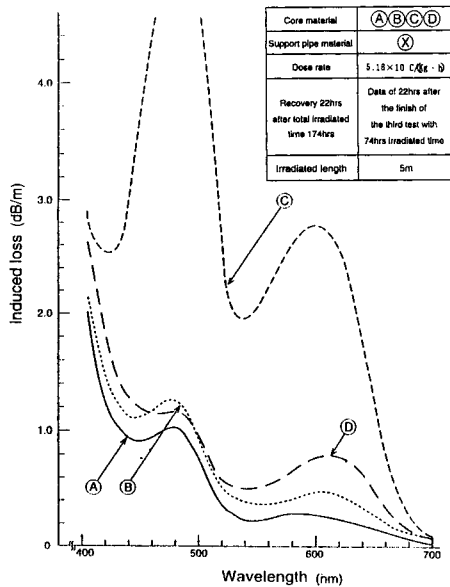


Fig. 5(c) Core materials dependence of radiation-induced losses of image guides after 22 hours from the end of the 3rd irradiation test (total irradiated time 174 hours).

during the recovery period after irradiation. During all three repeated irradiations, the radiation resistivity of sample D image guide, which uses a Cl-doped core, is much weaker than the samples with F-doped cores. However, sample D shows rapid recovery after irradiation, the induced loss being almost the same as samples A and B which use F-doped cores. Nevertheless, after the first recovery period, rapid deterioration was observed at the beginning of the second irradiation, reaching the induced loss value observed at the end of the first irradiation in a short time. Apart from sample D which is Cl-rich, other samples showed a small recovery after irradiation.

3. 2 Evaluation by average visual radiation-induced loss at visible wavelength

Image guides are used for remote visual observation, and are intended to be used, either directly or indirectly, by human eyes. With this in mind, we considered more practical methods to evaluate the radiation resistivity especially for image guides, rather than methods used for optical fibers which only evaluate the induced loss vs. wavelength relations.

Therefore, we introduce a calculation combining the spectral luminous efficiency, shown in Fig. 6, and the prevailing induced loss vs. wavelength characteristic. This method, which uses L (average visual radiation-induced loss) of visible wavelengths perceived by the human eye, enables a practical evaluation of degradation in picture quality caused by irradiation.⁷⁾ The output power vs. wavelength characteristic is calibrated in terms of the spectral luminous efficiency using a basic induced loss vs. wavelength characteristic, in the case of sample A of Fig. 3(a), This is shown in Fig. 7 along with the condition before irradiation (initial). The average visual radiation-induced loss L in the whole range of visible wavelengths with respect to spectral luminous efficiency is calculated by,

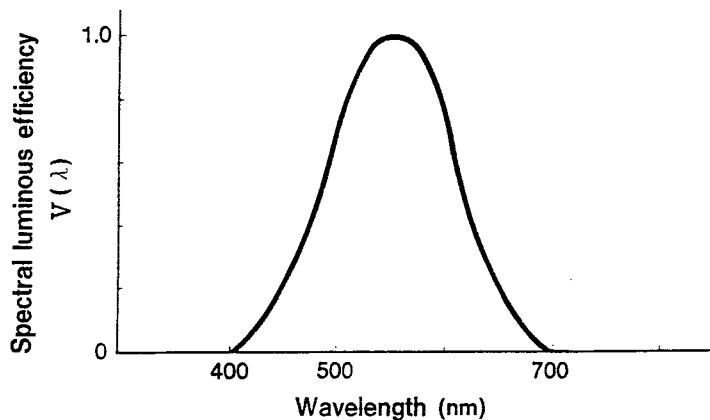


Fig. 6 Spectral luminous efficiency curve.

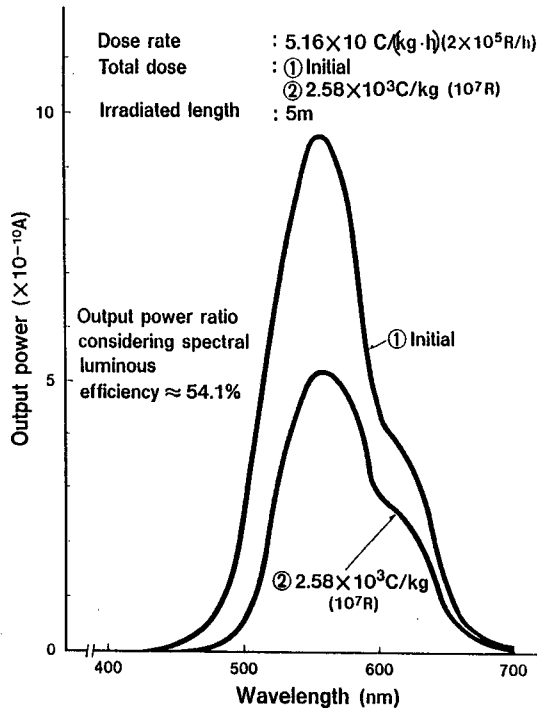


Fig. 7 Output power transferred by spectral luminous efficiency.

$$L(\text{db/m}) = -10/l \cdot \log(S_i/S_0) \quad (1)$$

where l is the irradiated length of the image guide (m). The smaller the value of (S_i/S_0) , the greater the deterioration in the image guide. On the other hand, as L becomes larger, the deterioration also becomes greater. Under the conditions of Table 2, an irradiation-recovery test was repeated three times. We plotted the data from this test on a graph which indicates the total irradiation time on the x-axis, and the average induced loss per 1 m obtained from formula (1) on the y-axis. The results are shown in Figs. 8, 9, 10 and 11 according to dose rates.

The results are summarized below.

1) The superiority for the radiation resistivity of image guides at the dose rates of $5.16 \text{ C}/(\text{kg}\cdot\text{h})$ ($2 \times 10^5 \text{ R/h}$) and $5.16 \times 10 \text{ C}/(\text{kg}\cdot\text{h})$ ($2 \times 10^6 \text{ R/h}$) is in the order of core materials $A > B > E > D > C$. Therefore, the order of the core dopant is $F > F + \text{OH} > \text{Cl} + \text{OH} > \text{OH}$.

2) At the dose rates of $1.29 \times 10^2 \text{ C}/(\text{kg}\cdot\text{h})$ ($5 \times 10^6 \text{ R/h}$) and $2.58 \times 10^2 \text{ C}/(\text{kg}\cdot\text{h})$ ($1 \times 10^6 \text{ R/h}$) the superiority order of core materials in image guides is, $A > B > E > C > D$. Therefore, the superiority order of the core dopant is $F > F + \text{OH} > \text{OH} > \text{Cl} + \text{OH}$.

3) As indicated in 1) and 2), radiation resistivity of samples C and D differs depending on the dose rate. This is accounted for by the fact that image guides with Cl-doped cores tend to recover rapidly after irradiation.

4) Image guides with F-doped cores have far superior radiation resistivity at any

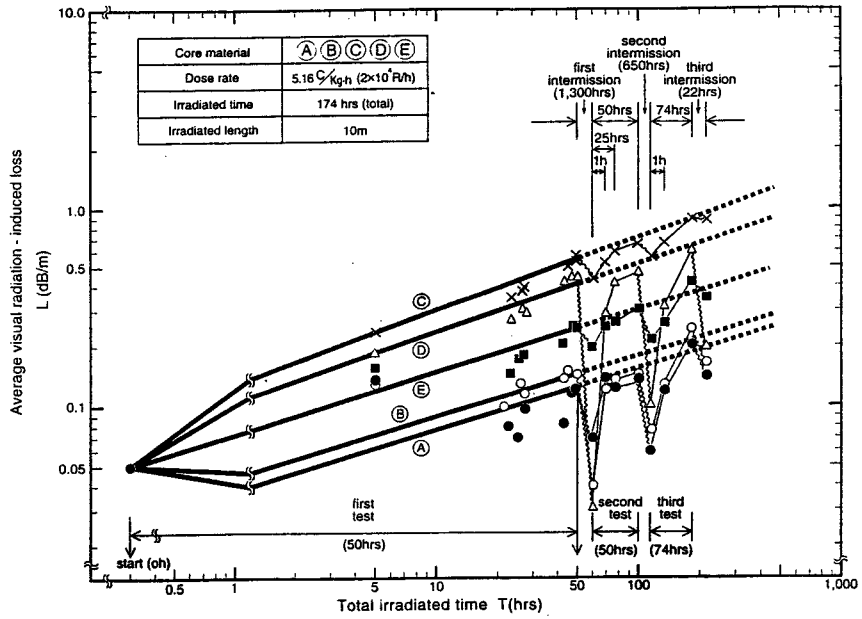


Fig. 8 Dependence of average visual radiation-induced losses on total irradiated time under the dose rate of $5.16 \text{ C}/(\text{kg}\cdot\text{h})$.

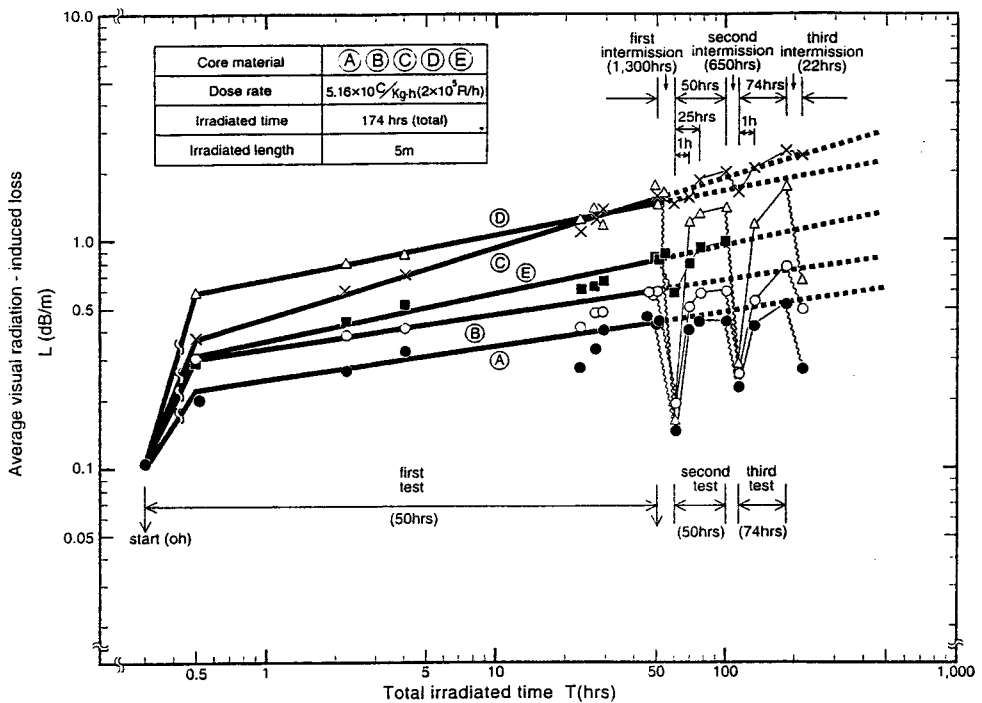


Fig. 9 Dependence of average visual radiation-induced losses on total irradiated time under the dose rate of $5.16 \times 10^6 \text{ C}/(\text{kg}\cdot\text{h})$.

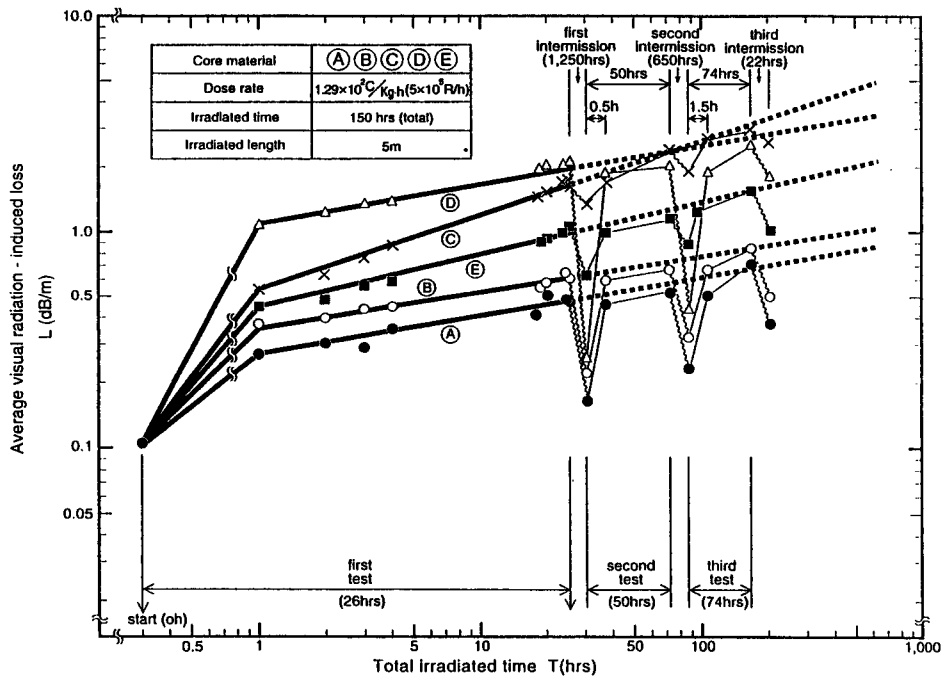


Fig. 10 Dependence of average visual radiation-induced losses on total irradiated time under the dose rate of $1.29 \times 10^2 \text{ C}/(\text{kg}\cdot\text{h})$

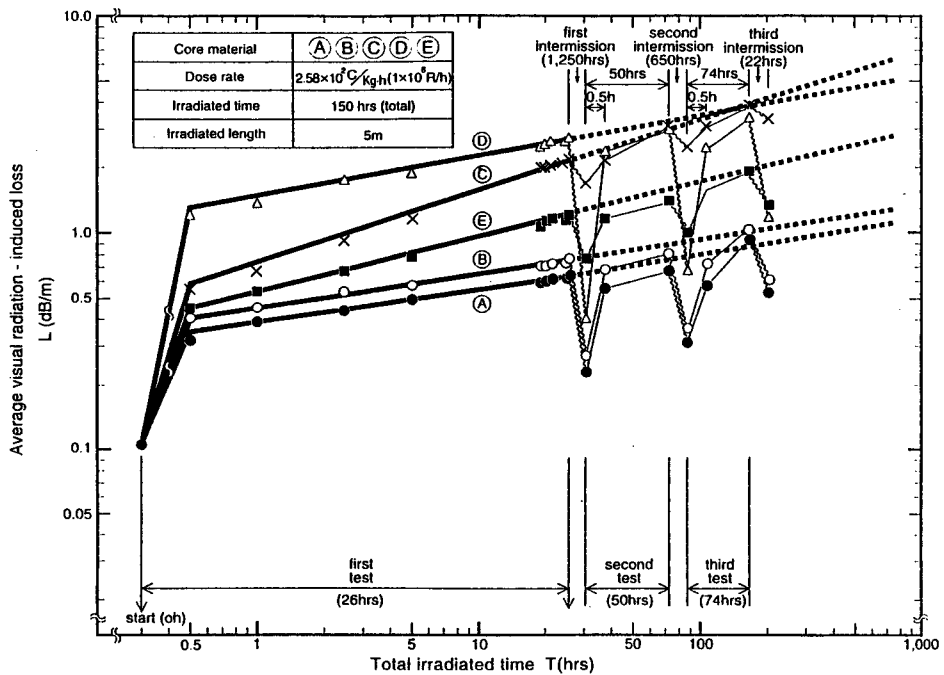


Fig. 11 Dependence of average visual radiation-induced losses on total irradiated time under the dose rate of $2.58 \times 10^2 \text{ C}/(\text{kg}\cdot\text{h})$

dose rate. Moreover, at dose rates above $5.16 \times 10^3 \text{ C}/(\text{Kg}\cdot\text{h})$ ($2 \times 10^6 \text{ R/h}$), or as the dose rate becomes higher, the superiority of the radiation resistivity of F-doped cores becomes more pronounced.

5) Sample D which uses a Cl-doped core, shows much more deterioration than those using F-doped cores, but as noted in 3), the sample shows rapid recovery after irradiation at any dose rate. On the other hand, image guide samples C and E which use OH-doped cores, show a small recovery after irradiation.

6) Judging solely from the average induced loss, repeatedly irradiated samples quickly reach the final deterioration level of the preceding irradiation. In other words, if the total irradiation time is the same, the radiation resistivity for repeated irradiation tests with time for recovery and that for continuous irradiation tests are about the same.

We conclude that the relation between $L(\text{dB}/\text{m})$ and $T(\text{hrs})$, as shown in Figs. 8-11, is not affected by irradiation methods, continuous or repeated irradiation. Therefore, the relation can be described by a formula $\log L = a \cdot \log T + b$. The constants a and b for each dose rate of core A are obtained by applying the least squares method. The results are as follows.

$$\text{dose rate } 5.16 \text{ C}/(\text{kg}\cdot\text{h}) \quad : \quad \log L = 0.221 \log T - 1.402 \quad (2)$$

$$\text{dose rate } 5.16 \times 10 \text{ C}/(\text{kg}\cdot\text{h}) \quad : \quad \log L = 0.1621 \log T - 0.623 \quad (3)$$

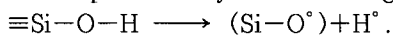
$$\text{dose rate } 1.29 \times 10^2 \text{ C}/(\text{Kg}\cdot\text{h}) \quad : \quad \log L = 0.1951 \log T - 0.558 \quad (4)$$

$$\text{dose rate } 2.58 \times 10^2 \text{ C}/(\text{kg}\cdot\text{h}) \quad : \quad \log L = 0.201 \log T - 0.436 \quad (5)$$

From the above equations, the value of L , during longer irradiation time can be predicted by extrapolation.

3.3 Radiation-induced defects in silica glass

Using samples A, B, C, D and E, we performed ESR spectroscopy to identify defects in the silica glass before and after irradiation ($2.58 \times 10 \text{ C}/(\text{kg}\cdot\text{h}) \times 50\text{h}$). The results are shown in Table 3.⁹⁾ For E' ($\equiv \text{Si}^\circ$) and NBOHC ($\equiv \text{Si}-\text{O}^\circ$), we measured the spin density per unit weight, but the PORC ($\equiv \text{Si}-\text{O}-\text{O}^\circ$) generation was so small that we have only indicated whether it was present or not. Before irradiation, neither NBOHC nor PORC could be detected in any of the core materials. Table 3 shows that of the defects caused by irradiation; E' is the largest in value. The spin density of E' is the largest in core material D, and then C. This shows good agreement with the radiation resistivity characteristics we have already determined. Table 3 also shows that the generation of NBOHC has relations with the presence of OH. It is believed that NBOHC is produced by the following reaction:



Additionally, it has been reported that the absorption at wavelengths between 600-630 nm is caused by NBOHC.⁹⁾

Table 3 Results of ESR measurement

Core Material	Initial	After the irradiation test [2.58×10^2 C/kg·h(1×10^6 R/h) \times 50h]		
	Spin density of E' (Si' [·]) (spins/g)	Spin density of E' (Si' [·]) (spins/g)	Spin density of NBOHC(Si-O' [·]) (spins/g)	Presence of PORC (Si-O-O' [·])
A	4.3×10^{13}	5.1×10^{15}	6.1×10^{12}	no
B	4.4×10^{13}	7.0×10^{15}	2.4×10^{13}	no
C	————*	1.3×10^{16}	4.4×10^{14}	yes
D	5.9×10^{13}	9.7×10^{16}	7.7×10^{13}	no
E	————*	3.1×10^{16}	7.9×10^{13}	yes

* Below the limit of inspection ($< 1.8 \times 10^{13}$)

However, considering the movements of the irradiation induced loss shown in Figs. 3 (a)-5(c), it can be assumed that the absorption around 480 nm, which is closely related to the presence of OH, may also be attributed to the presence of NBOHC.

It is obvious that the radiation resistivity is closely related to radiation defects E' and NBOHC in the glass.

4. Conclusion

The results of intermittent irradiation tests were identical to the continuous irradiation tests, in that the image guides with F-doped core showed most superior resistivity at all the four dose rates. The same results were obtained from the induced loss characteristics and also from the average visual radiation-induced loss at visible wavelengths.

The induced loss quickly reached the final deterioration level of the preceding irradiation. Therefore, we can assume that for the same dose rate, the deterioration caused by irradiation is basically affected by the total irradiation time and that the recovery process does not affect it. However, even though image guides using Cl-doped cores deteriorate far more than F-doped core materials, they tend to recover quickly after irradiation at any dose rate. This is the reason why image guides using Cl-doped cores showed only slightly more deterioration under continuous irradiation compared to intermittent irradiation.

From the relation between the defects produced in silica glass by irradiation and the induced loss, it is clear that E' and NBOHC have a large influence on the radiation resistivity. F-doped cores which have far more superior radiation resistivity, have a much smaller spin density value of E' and NBOHC caused by irradiation than OH-doped and Cl-doped cores.

References

- 1) H. Hayami, T. Shintani, K. Suzuki and T. Ishitani, SPIE Vol. 992, Fiber Optics Reliability; Benign and Adverse Environments, II, 60 (1988).
- 2) K. Yahagi, J. At. Energy Soc. Jpn., (in Japanese), **27**, 768 (1985).
- 3) T. Kakuta, et al., Papers Tech. Mtg., Electrical Insulating Material (in Japanese), EIM-85-30 (IEE Japan) 37 (1985).
- 4) K. Ara, et al., National Conf. Record, Semi-Conductor Devices and Materials of IEICE (in Japanese), No. **339**, 1 (1985).
- 5) T. Ohnishi, S. Okamoto, T. Kanazawa, Y. Tsujii, H. Hayami, T. Ishitani, T. Akutsu and K. Suzuki, Bull. Univ. Osaka Prefect. A, **39**, 45 (1990).
- 6) S. Okamoto, T. Ohnishi, T. Kanazawa, Y. Tsujii, H. Hayami, T. Ishitani, T. Akutsu and K. Suzuki, Bull. Univ. Osaka Prefect. A, **40**, No. 1, 183 (1991).
- 7) S. Okamoto, T. Ohnishi, T. Kanazawa, Y. Tsujii, H. Hayami, T. Ishitani, O. Kishihara and K. Suzuki, Ann. Rep. Osaka Prefect. Radiat. Res. Instit., **30**, 51 (1990).
- 8) H. Hayami, T. Akutsu, T. Ishitani and K. Suzuki, J. Nucl. Sci. Tech., **30**, No.2, 95 (1993).
- 9) K. Nagasawa, New Glass, **4**, No.1, 51 (1989).